Cell

A Dynamic Epicardial Injury Response Supports Progenitor Cell Activity during Zebrafish Heart Regeneration

Alexandra Lepilina,[1,3] Ashley N. Coon,[1,3] Kazu Kikuchi,[1] Jennifer E. Holdway,[1] Richard W. Roberts,[1] C. Geoffrey Burns,[2] and Kenneth D. Poss[1,*]
[1] Department of Cell Biology, Duke University Medical Center, Durham, NC 27710, USA
[2] Cardiovascular Research Center, Massachusetts General Hospital, Charlestown, MA 02129, USA
[3] These authors contributed equally to this work.
*Contact: k.poss@cellbio.duke.edu
DOI 10.1016/j.cell.2006.08.052

SUMMARY

Zebrafish possess a unique yet poorly understood capacity for cardiac regeneration. Here, we show that regeneration proceeds through two coordinated stages following resection of the ventricular apex. First a blastema is formed, comprised of progenitor cells that express precardiac markers, undergo differentiation, and proliferate. Second, epicardial tissue surrounding both cardiac chambers induces developmental markers and rapidly expands, creating a new epithelial cover for the exposed myocardium. A subpopulation of these epicardial cells undergoes epithelial-to-mesenchymal transition (EMT), invades the wound, and provides new vasculature to regenerating muscle. During regeneration, the ligand *fgf17b* is induced in myocardium, while receptors *fgfr2* and *fgfr4* are induced in adjacent epicardial-derived cells. When fibroblast growth factors (Fgf) signaling is experimentally blocked by expression of a dominant-negative Fgf receptor, epicardial EMT and coronary neovascularization fail, prematurely arresting regeneration. Our findings reveal injury responses by myocardial and epicardial tissues that collaborate in an Fgf-dependent manner to achieve cardiac regeneration.

INTRODUCTION

Progenitor cell populations have been identified within most mammalian organs, including skin, blood, bone, reproductive tissues, skeletal muscle, kidney, lung, liver, intestine, heart, and brain. These cells vary widely in frequency, developmental potential, and the ability to regenerate damaged or lost tissue. The most highly regenerative is the multipotent hematopoietic stem cell (HSC). A single HSC can reconstitute the entire hematopoietic system of an irradiated mammal (Wagers et al., 2002; Shizuru et al., 2005). By contrast, progenitor cells within the majority of mammalian organs restore those cells lost in the course of normal organ function or after minor injury, but cannot regenerate after major damage or removal of structures.

Ischemic myocardial infarction causes irreversible cell loss and scarring and is a major source of morbidity and mortality in humans. Thus, the inability to replace damaged cardiac muscle ranks among the most prominent regenerative failures of mammals (Rubart and Field, 2006). Recent attempts to identify cardiac progenitor cells have revealed at least three rare cell populations with the potential to generate new cardiomyocytes (CMs) postnatally (Beltrami et al., 2003; Cai et al., 2003; Oh et al., 2003, Laugwitz et al., 2005). c-kit^{pos}Lin^{neg} cells and islet1^{pos} cells both exist normally as undifferentiated or poorly differentiated cells but will differentiate to a contractile phenotype under in vitro conditions. Moreover, islet1^{pos} cells were shown by genetic lineage tracing experiments to give rise to a large percentage of CMs during development and growth, while c-kit^{pos}Lin^{neg} cells contributed new CMs when injected into rodent myocardial infarcts. The discoveries of cardiac progenitor cells have exciting implications for cardiac biology and disease. Yet, it is unclear why they fail to support natural regeneration after ischemic infarction or other injury paradigms.

Regeneration is an evolutionarily conserved feature of vertebrate species. Nonetheless, selected nonmammalian vertebrates, including urodele amphibians and teleost fish, display an elevated regenerative spectrum, with many more tissues capable of impressive regeneration. For instance, certain newts or axolotls can regenerate limbs, tail, spinal cord, retina, lens, jaws, portions of intestine, and brain tissue. Also, these animals achieve a partial regenerative response after mechanical damage to the cardiac ventricle. Cell-cycle entry and mitoses are observed in spared CMs, along with scarring (Oberpriller and Oberpriller, 1974). Because related urodeles or

teleosts can display marked interspecies differences in regeneration of their appendages, it is believed that the capacity for regeneration is an ancestral condition that has occasionally been attenuated in the course of vertebrate evolution (Scadding, 1977; Wagner and Misof, 1992). Thus, most biologists suspect that machinery to optimize regeneration from progenitor cells is present but lies dormant in mammals.

By contrast with mammals, teleost zebrafish regenerate cardiac muscle after major injury; therefore, study of this process can illuminate how heart regeneration is naturally optimized. Following resection of the apex of the zebrafish ventricle, CM hyperplasia vigorously renews the myocardium and restricts scar formation (Poss et al., 2002; Raya et al., 2003). Very little is known about cellular and molecular mechanisms of this process, including whether an undifferentiated progenitor cell type contributes or how nonmyocardial cell types participate. Over the past several years, large-scale genetic screens (Chen et al., 1996; Stainier et al., 1996), transgenic reporter strains (Lawson and Weinstein, 2002), and lineage studies (Keegan et al., 2005) have revealed critical aspects of cardiovascular development in zebrafish embryos. Some molecular mechanisms are likely to be shared by embryonic cardiogenesis and adult cardiac regeneration (e.g., myocardial differentiation programs). However, heart regeneration invokes multiple distinct and defining events, including (1) initiation by injury, (2) activation of quiescent tissue, (3) ostensibly local development as opposed to organ- and organism-wide development, (4) simultaneous healing and growth, (5) morphogenesis on a larger scale to form adult tissue, and (6) possible long-term maintenance or de novo creation of progenitor cells.

Here, to identify and characterize key processes responsible for cardiac regeneration in zebrafish, we employed transgenic reporter strains, identified new molecular markers for regenerating tissues, and performed genetic loss-of-function studies. Our findings reveal dynamic, coordinated cellular and molecular events that mediate heart regeneration.

RESULTS

Heart Regeneration Involves Changes in Myocardial Differentiation

A hallmark of many regenerating systems, from the decapitated planarian to the amputated amphibian limb, is formation of the regeneration blastema, a proliferative mass of undifferentiated progenitor cells from which new differentiated structures arise (Reddien and Sanchez-Alvarado, 2004; Brockes and Kumar, 2005). Previous studies did not investigate whether myocardial regeneration in zebrafish utilizes a blastema or instead results purely from expansion of existing CMs without changes in differentiation (Poss et al., 2002; Raya et al., 2003).

To sensitively monitor changes in myocardial differentiation during heart regeneration, we used transgenic zebrafish expressing a nuclear-localized DsRed2 fluorescent reporter for *cmlc2* (*cmlc2:nRFP*, where RFP is red fluorescent protein). Individual differentiated CMs were predicted to show high levels of nuclear fluorescence (RFP^{hi}), while less differentiated or transitioning CMs should display lower fluorescence (RFP^{lo}). As expected, CM nuclei in uninjured ventricles were uniformly RFP^{hi}, as were those in ventricles at 3 days after amputation (dpa; Figure 1A). However, by 14 dpa and as early as 7 dpa, CM nuclei with dramatically lower RFP fluorescence appeared at the apex. RFP^{lo} cells were typically most abundant at 22 dpa, at which time what appeared to be the entire regenerate could in some cases be distinguished (Figure 1A). By 30 dpa, when a contiguous ventricular wall was restored in our experiments, CM differentiation as assessed by the reporter strain had recovered to normal or near-normal levels (Figure 4D). Thus, heart regeneration involves demonstrable changes in myocardial differentiation.

New Myocardium Arises from Undifferentiated Progenitor Cells

Analyses of *cmlc2:nRFP* animals at multiple times postresection suggested a mechanism in which undifferentiated cells accumulate in the wound and differentiate into contractile CMs. To confirm this mechanism, we examined the developmental timing of myocardial differentiation using double transgenic animals with both nRFP and enhanced green fluorescent protein (EGFP) driven by *cmlc2* promoters. This approach takes advantage of the different properties of these fluorescent proteins and can reveal temporal and spatial characteristics of promoter activation and inactivation (Verkhusha et al., 2001; Verkhusha et al., 2003). EGFP folds and fluoresces more rapidly than DsRed2 (Baird et al., 2000; Bevis and Glick, 2002)—approximately one day faster in embryonic zebrafish CMs activating the *cmlc2* promoter for the first time (Figure S1). EGFP is also less stable than DsRed2 and degrades about twice as rapidly in vitro and in vivo (Verkhusha et al., 2003). This bidirectional developmental timer allows us to (1) identify new CMs arising from an undifferentiated state ($EGFP^{pos}RFP^{neg}$ cells), and (2) determine whether once-expressing CMs have switched off the *cmlc2* promoter as part of the regeneration program ($EGFP^{neg}RFP^{pos}$ cells).

In injured double transgenic ventricles, we never observed $EGFP^{neg}RFP^{pos}$ myocardium (n = 931 apical CMs examined from 12 animals at 3 and 7 dpa), indicating that the RFP^{lo} cells do not result from a loss of the differentiated state. At 3 and 4 dpa, myocardium was uniformly $EGFP^{pos}RFP^{pos}$, including the apical edge of the regenerate. At 5 dpa, myocardial tissue at the resection plane began to display some areas of $EGFP^{pos}RFP^{neg}$ tissue (Figure 1B; Table S1). Strikingly, at 7 dpa, the apical myocardial edge was uniformly $EGFP^{pos}RFP^{neg}$, indicative of a front of CMs newly differentiating from a noncontractile state (Figure 1B). This $EGFP^{pos}RFP^{neg}$ front was also present at 14 dpa but apically shifted (data not shown). Similar results were observed with a double transgenic strain

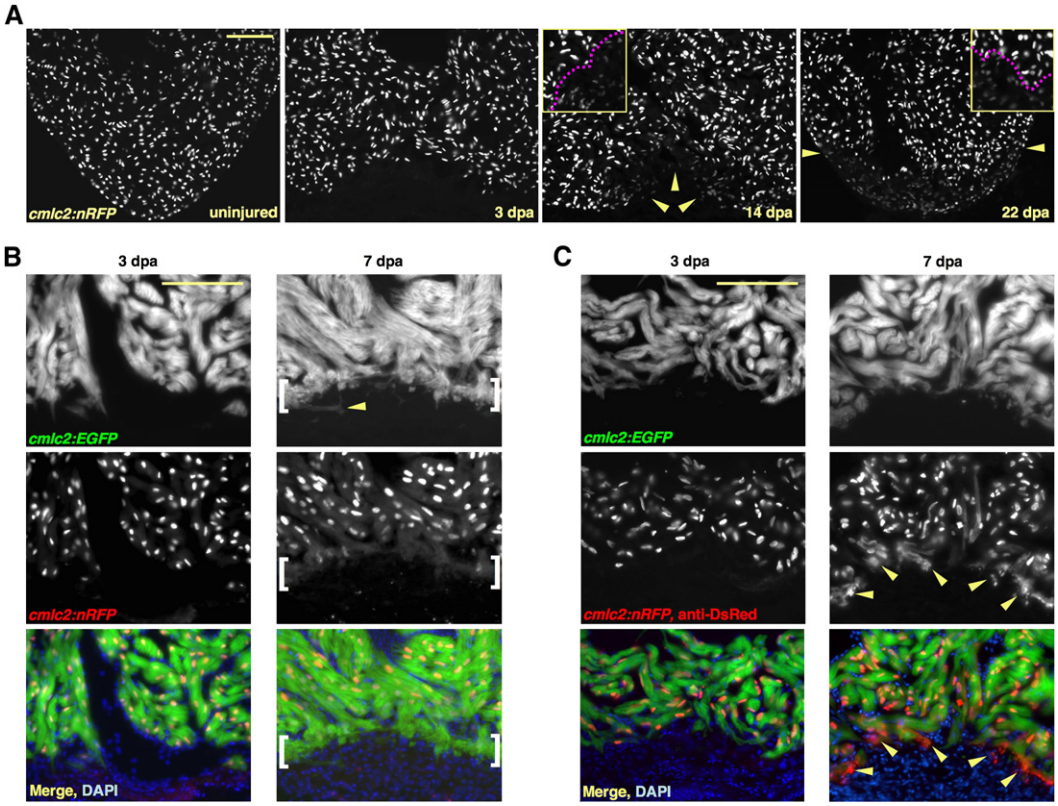

Figure 1. New Myocardium Arises from Undifferentiated Progenitor Cells

(A) Sections through uninjured and injured *cmlc2:nRFP* ventricles. A subpopulation of RFP^{lo} nuclei manifests by 14 dpa (arrowheads), representing ostensibly the entire regenerate by 22 dpa. Magenta line in high-magnification insets delineates RFP^{hi} CMs (above line) from RFP^{lo} CMs.

(B) *cmlc2:nRFP; cmlc2:EGFP* ventricles. EGFP and RFP expression from the *cmlc2* promoter is reported at the same basoapical level at 3 dpa. By 7 dpa, an RFP^{neg} front of newly differentiated muscle reporting the faster-fluorescing EGFP (brackets) appears apical to the $EGFP^{pos}RFP^{pos}$ portion. Arrowhead indicates an $EGFP^{pos}$ cell process extending into the clot.

(C) *cmlc2:nRFP; cmlc2:EGFP* ventricles stained for DsRed immunoreactivity with an anti-DsRed antibody. At 3 dpa, there is no difference in appearance from the unstained 3 dpa ventricle in (B). By 7 dpa, a front of RFP^{cyto} muscle (arrowheads), representing the most recently differentiated CMs, colabels $EGFP^{pos}$ tissue apical to natural RFP^{nuc} fluorescence. Scale bar = 100 μm.

reporting *nRFP* from the *cmlc2* promoter and *EGFP* from the promoter for *β-actin 2*, another gene expressed strongly in CMs (data not shown). These results indicated that regenerating myocardium matures from undifferentiated, Cmlc2-negative cells established at the amputation plane within 5 days of apical resection.

We confirmed this finding with an additional developmental timing assay using an antibody against DsRed. A previous study using transgenic *Drosophila* embryos expressing DsRed behind the *hedgehog* promoter found that DsRed immunoreactivity is detectable many hours before and anterior to natural RFP fluorescence during posterior-to-anterior differentiation of eye ommatidia (Akimoto et al., 2005). Sections of 3 dpa *cmlc2:nRFP*; *cmlc2:EGFP* ventricles stained with the anti-DsRed antibody appeared identical to unstained sections (Figures 1B and 1C). However, DsRed immunoreactivity apical to natural RFP fluorescence was detectable as early as 4–5 dpa, labeling precisely the $EGFP^{pos}RFP^{neg}$ apical edge of the regenerate at 7 dpa (Figure 1C; Table S1). Thus, new myocardium matures from an undifferentiated population of progenitor cells.

Cardiac Progenitors Initiate a Wave of Regenerative Morphogenesis

Serendipitously, CMs at the apical edge of the regenerate displayed a conspicuous cytosolic RFP (RFP^{cyto}) profile when stained with the anti-DsRed antibody, representing nonfluorescent RFP translation product that is slow to fold and accumulate in the nucleus. In regenerating hearts, RFP^{cyto} CMs were absent at 3 dpa and rare at 4 dpa. By 5 and 7 dpa, large, RFP^{cyto} CMs were abundant within a contiguous front at the apical edge of the regenerate (Figure 1C; Table S1). We suspected that RFP^{cyto} cells were freshly differentiated CMs activating the *cmlc2* promoter for the first time, and we tested this idea with embryonic *cmlc2:nRFP* hearts. As predicted, 24 hpf embryonic CMs (having no natural RFP fluorescence) showed a full RFP^{cyto} profile and 48 hpf hearts had a subset of RFP^{cyto} CMs among mostly RFP^{nuc} CMs, while

60 hpf CMs displayed essentially complete nuclear RFP localization (Figure S2). This similarity in DsRed maturation kinetics between early CMs of the adult regenerate and of the embryonic heart suggested that a precardiac field akin to the embryonic heart field is formed and bears new CMs during cardiac regeneration.

In the embryonic zebrafish heart field, cardiac progenitors are identified by their expression of transcriptional activators of myocardial differentiation in lateral plate mesoderm several hours before induction of *cmlc2* (Chen and Fishman, 1996; Griffin et al., 2000; Yelon et al., 2000). We found that *nkx2.5*, *hand2*, and *tbx20*, the earliest markers of the embryonic zebrafish heart field, were also the earliest detectable precardiac markers during heart regeneration. *hand2* was detectable by in situ hybridization (ISH) in cells coating the apical myocardial edge at 3 dpa, while *nkx2.5* and *tbx20* were first detectable in a similar population lining the existing muscle by 4 dpa. Because of their localization and emergence prior to evidence of significant new CM differentiation (Figure 2A; Table S1), these *hand2*/*nkx2.5*/*tbx20*-positive cells most likely represent progenitor cells that have recently acquired a cardiac fate. A domain of conspicuously enhanced expression of these markers as well as other transcriptional activators Mef2 and *tbx5* was present at the apical edge of the regenerate at 5 and 7 dpa, correlating with the differentiating front of new CMs defined by developmental timing assays (Figure 2B; Table S1).

Previous studies showed that proliferation of CMs is a prominent feature of zebrafish heart regeneration, initiated around 7 dpa and peaking by 14 dpa (Poss et al., 2002). Indeed, a significant amount of myocardial regeneration occurs in the second week after resection (Figure 2). We observed RFP^{cyto} CMs at the apical edge of the regenerate at 14 dpa, mainly comprised of smaller CMs that most likely contribute compact myocardium of the ventricular wall (Figure 2C). A domain of enhanced precardiac marker expression was also detectable here at 14 dpa, becoming less prominent as regeneration progressed (Figure 2C; Table S1). To determine whether cardiac progenitors facilitate CM proliferation during regeneration, we labeled *cmlc2:nRFP* animals with BrdU at 7 or 14 dpa and assessed CM differentiation using the anti-DsRed antibody. At 7 dpa, BrdU labeling was specific to freshly differentiated, RFP^{cyto} CMs, with little or no incorporation in established RFP^{nuc} CMs. At 14 dpa, BrdU incorporation was seen in both RFP^{nuc} and RFP^{cyto} CMs (Figure 2D). Thus, our data indicate that the precardiac field is a source of CMs with the capability to proliferate and carry out regeneration. This finding is consistent with our previous study in which we identified the apical edge as a proliferative front during regeneration (Poss et al., 2002).

In total, our experiments reveal that new myocardium forms from an undifferentiated field comparable to a blastema, comprised of progenitor cells that associate with existing myocardium within 3–4 days of injury, activate expression of precardiac markers, and differentiate into proliferative CMs. After this initial seeding of progenitor cells, regenerative morphogenesis proceeds in a basal-to-apical wave of progenitor cell seeding, maturation, and proliferation.

Cardiac Injury Activates the Entire Epicardial Cell Layer

Another hallmark of many regenerating systems is emergence of a multi-layered epithelial structure called the wound (or regeneration) epidermis, which forms over the blastema by migration of spared epithelial cells. For example, in the regenerating fin, epidermal and blastemal tissues interact throughout regeneration to catalyze morphogenesis, events that involve epidermal synthesis and blastemal reception of growth factors (Poss et al., 2000). We predicted that regenerating myocardium would require interaction with the epicardium, an easily distinguishable epithelial cell layer that envelops all peripheral surfaces of the heart and influences myocardial development in the embryo. To assess epicardial activity during regeneration, we followed expression of *raldh2* and *tbx18*, genes expressed in the developing embryonic epicardium (Moss et al., 1998; Kraus et al., 2001).

Epicardial cells of the uninjured adult heart showed little or no expression of *raldh2*, which encodes the rate-limiting enzyme for retinoic acid (RA) synthesis. Surprisingly, as early as 24 hr after partial ventricular amputation (hpa), *raldh2* was strongly induced in epicardium surrounding the ventricle, atrium, and outflow tract (Figure 3A). Induced expression of *raldh2* appeared sequentially, first in the outflow tract and atrial epicardium by 6–12 hpa and then joined by the ventricular epicardium (data not shown). Ventricular and atrial epicardial cells also expressed *tbx18* by 1–2 dpa (Figure 3B) and began to proliferate (Figure 3C). BrdU-labeling experiments demonstrated robust, S phase entry of most *raldh2*/*tbx18*-positive epicardial cells at 3 dpa. By 7 dpa, this response began to localize to the injured ventricular apex, where BrdU-labeled epicardial cells enclosed the wound (Figures 3C and 3D). By 14 dpa, activated epicardium was confined to the wound (Figures 3A, 3B, and 3D). Thus, a focal ventricular injury stimulates organ-wide, developmental activation of the adult zebrafish epicardium, the expansion of which creates an epithelial cover for regenerating myocardium.

Epicardial-Derived Cells Invade and Vascularize the Regenerating Myocardium

Epicardial cells at the apex of the injured ventricle not only enveloped the wound but also displayed a remarkable invasive behavior. While *raldh2* expression began to subside in epicardial cells by 14 dpa, a large number of cells retained *tbx18* expression and integrated into the wound and new muscle. Even by 30 dpa, many *tbx18*-positive cells were maintained in the regenerate (Figure 3D). These invasion events were reminiscent of embryonic heart development, during which epicardial cells undergo epithelial-to-mesenchymal transition (EMT) and invade the

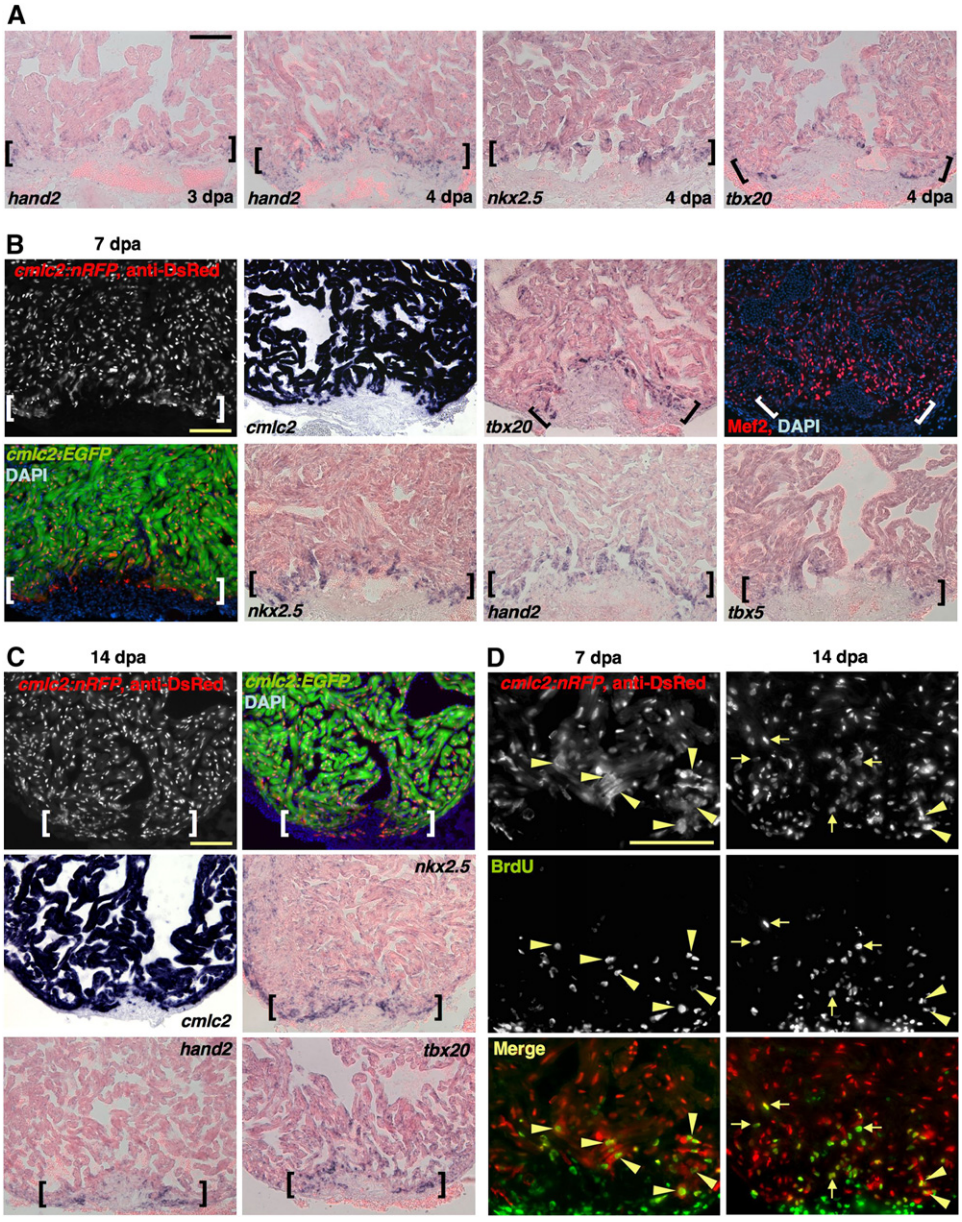

Figure 2. A Precardiac Field Is Established during Regeneration and Supports CM Proliferation

(A) The precardiac marker *hand2* is expressed in cells coating the apical edge of the existing muscle at 3 dpa (violet stains). At 4 dpa, *nkx2.5* and *tbx20* are also expressed in cells distributed along the resection plane. By contrast, no new CM differentiation events are detected by anti-DsRed staining in *cmlc2:nRFP* zebrafish at 3 dpa (see Figure 1) and only sparse events at 4 dpa (Table S1). The pink background represents myocardial autofluorescence, which aids visualization of positive signals.

(B) *nkx2.5*, *tbx20*, *hand2*, *tbx5*, and Mef2 (red nuclear stain) are each present in a domain of enhanced expression at the apical edge of the regenerate (brackets), an area of most recent myocardial differentiation events as assessed in the *cmlc2:nRFP; cmlc2:EGFP* strain. The ISH pattern of *cmlc2* at 7 dpa is also shown to indicate differentiated muscle.

(C) By 14 dpa, freshly differentiated RFP^{cyto} cells in *cmlc2:nRFP; cmlc2:EGFP* hearts appear smaller and remain at the apical edge as regeneration proceeds (brackets). Enhanced *nkx2.5, tbx20*, and *hand2* expression remains detectable in this region.

(D) Seven (left) and 14 dpa (right) ventricles from *cmlc2:nRFP* zebrafish stained for DsRed immunoreactivity (red) and BrdU incorporation (green). At 7 dpa, BrdU label is detectable only in newly differentiated RFP^{cyto} cells (arrowheads). By 14 dpa, BrdU is also detectable in RFP^{nuc} CMs (arrows). Scale bar = 100 μm.

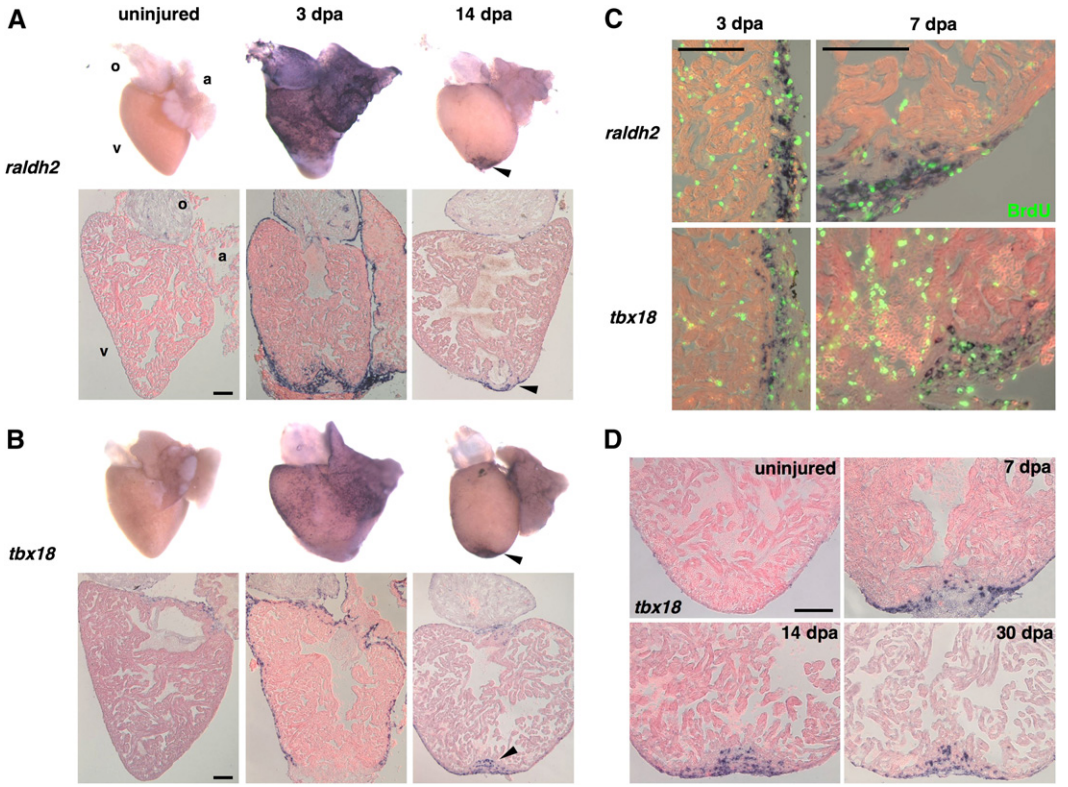

Figure 3. Organ-Wide Activation of Epicardial Cells and Invasion of the Regenerate

(A and B) Whole-mount (top) and section (bottom) ISH of uninjured and 3 and 14 dpa hearts for *raldh2* (A) and *tbx18* (B). Expression of each marker is low or undetectable in the uninjured hearts but induced at 3 dpa in epicardial tissue surrounding the atrium (a) and ventricle (v) for *tbx18* and these tissues plus the outflow tract (o) for *raldh2*. The endocardium surrounding wounded myofibers also expresses *raldh2*. By 14 dpa, expression of both markers is localized to the apical wound (arrowhead).

(C) Colocalization of BrdU (green) with *raldh2* (top) and *tbx18* (bottom) in the ventricular epicardium at 3 and 7 dpa. The left images display a lateral edge of the 3 dpa ventricle away from the wound, while the right images display a lateral and apical portion of the 7 dpa ventricle including some of the wound. By 7 dpa, *raldh2*/*tbx18*/BrdU-positive cells begin to localize to the injury site. The majority of nonepicardial BrdU-positive cells are erythrocytes within the ventricular lumen.

(D) Epicardial-derived cells positive for *tbx18* invade the regenerate by 7 dpa and remain by 30 dpa. Scale bar = 100 μm.

subepicardial space and myocardium. Following these EMT events, epicardial-derived cells generate endothelial and smooth muscle cells of the subepicardial and coronary vasculature (Dettman et al., 1998; Olivey et al., 2004).

To identify vascular changes during heart regeneration, we used *fli1:EGFP* transgenic zebrafish that report fluorescence in endothelial cells. Coronary vasculature was easily distinguishable from the endocardial endothelium by its location, shape, and stronger intensity of fluorescence (Figure 4A) and was similarly distinguishable in ventricles of *flk1:EGFP* transgenic zebrafish (data not shown). We found an extensive network of new coronary vessels in *cmlc2:nRFP; fli1:EGFP* regenerates by 14 dpa, coincident with the appearance of epicardial-derived cells. This coronary plexus penetrated regions of differentiating RFP^{lo} CMs at 14 dpa and was stably maintained in 30 dpa regenerates (Figures 4B–4D). Our results indicate that developmentally activated epicardial cells invade the new myocardium and create a dense vascular network likely to encourage regeneration.

Fgf Signaling Promotes Epicardial EMT and Coronary Neovascularization, Facilitating Myocardial Regeneration

Why do activated epicardial cells preferentially penetrate and vascularize regenerating myocardium? In vitro studies have shown that fibroblast growth factors (Fgfs) promote epicardial EMT into collagen gels (Morabito et al., 2001). To determine whether Fgfs help recruit epicardial cells into cardiac wounds and regenerating muscle, we examined expression by ISH of multiple Fgf ligands and all 4 Fgfr receptors (Fgfrs) during regeneration. *fgf17b*, a member of the Fgf8/17/18 subclass of Fgf ligands (Cao et al., 2004), was the only ligand gene that showed detectable expression among several we tested (Figure 5A). In uninjured and 3 dpa ventricles, *fgf17b* was faintly detectable in cardiac myofibers. By 7 dpa, expression of *fgf17b* mRNA was strongly enhanced in CMs at the apical edge of the regenerate. Other cell types within the injury also expressed *fgf17b* at this stage. This augmented expression persisted at 14 dpa; by 30 dpa, the new

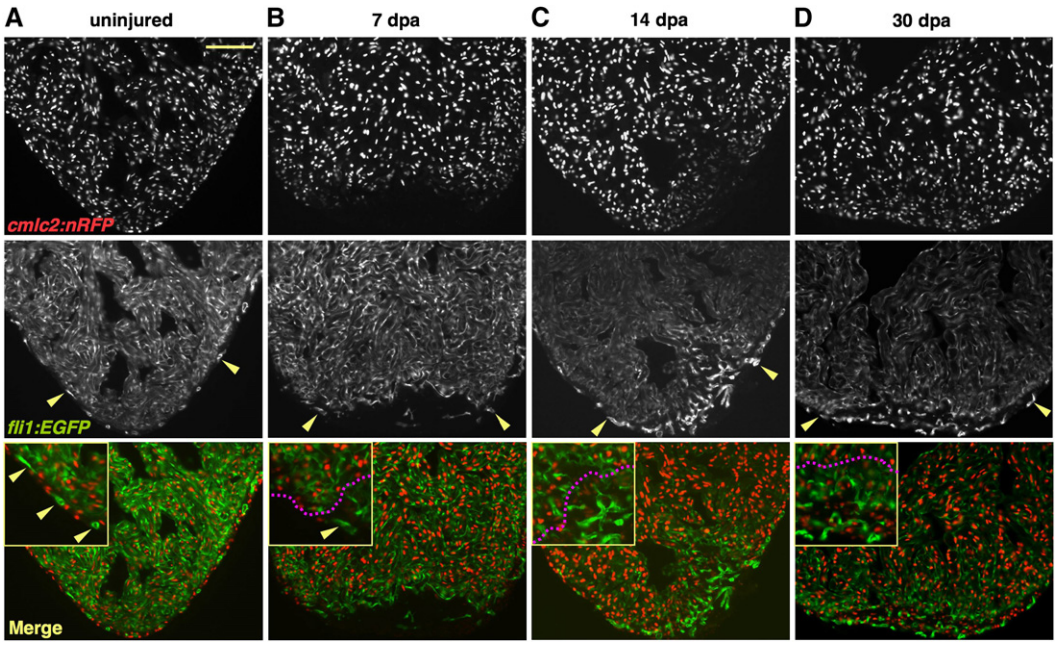

Figure 4. Enrichment of Coronary Vasculature during Regeneration

cmlc2:nRFP; fli1:EGFP ventricles displaying RFP fluorescence in CM nuclei (top) and EGFP in endocardial and vascular endothelial cells (middle).

(A) Weak EGFP fluorescence is emitted from endocardial cells that surround internal trabecular myofibers, while more intense fluorescence is reported in endothelial cells of the coronary vasculature (arrowheads).

(B) As early as 7 dpa, coronary vasculature begins to appear in the wound. Magenta line in high magnification inset delineates RFP^{hi} CMs (above line) from RFP^{lo} CMs.

(C) By 14 dpa, regenerating myocardium, identifiable as RFP^{lo}, is heavily vascularized.

(D) Myocardial differentiation has essentially recovered by 30 dpa, and the apical regenerate retains an extensive coronary network. Scale bar = 100 μm.

myocardial wall contained many cells with enhanced *fgf17b* expression.

Among zebrafish Fgf ligands, Fgf17b shows the highest homology to mammalian Fgf17, which binds receptors Fgfr1-3 (the "c" spliced forms) and Fgfr4 (Olsen et al., 2006). In the uninjured adult zebrafish heart, smooth muscle cells in the outflow tract expressed *fgfr1* and *fgfr2*, and valve mesenchyme expressed *fgfr1*, *fgfr2*, and *fgfr4* (data not shown). We did not detect by ISH expression of any *fgfrs* in the uninjured ventricular myocardium, nor did this tissue express *fgfrs* after injury. Interestingly, we detected expression of *fgfr2* and *fgfr4*, but not other *fgfrs*, in epicardial tissue during regeneration. *fgfr4* was expressed in rare epicardial cells around the periphery of the uninjured ventricle (Figure 5C). By 3 dpa, *fgfr4* was expressed in a slightly greater number of ventricular epicardial cells, although no cells in the wound expressed *fgfrs* at this time (data not shown). More remarkable was the expression of *fgfr2* and *fgfr4* in contiguous stretches of atrial epicardial cells at 3 dpa, far removed from the injury and reminiscent of *raldh2* and *tbx18* patterns (Figure S3). As regeneration continued, expression of these receptors resembled that of *tbx18* in particular, and, using double ISH, we found that *fgfr4* was expressed in a subpopulation of *tbx18*-positive cells adjacent to the apical edge of the regenerate (Figure S3). By 7 dpa, *fgfr2* and *fgfr4* were induced in epicardial cells within or at the lateral edges of wounds. By 14 dpa, each receptor was expressed in cells that had integrated into the wound and regenerating muscle, expression that persisted within the regenerate at 30 dpa (Figures 5B and 5C). Together, the temporal and spatial expression patterns of these genes suggested that Fgf17b released from the regenerating myocardium signals to *fgfr2/4*-expressing, epicardial-derived cells.

To directly test the function of Fgf signaling during cardiac regeneration, we used animals transgenic for a heat-inducible, dominant-negative Fgfr tagged with EGFP (*hsp70:dn-fgfr1*). In a previous study, we found that daily heat treatments of *hsp70:dn-fgfr1* animals effectively prevent regeneration of amputated fins (Lee et al., 2005). Furthermore, a single heat shock strongly and uniformly induced *dn-fgfr1* transgene expression in cardiac cells for more than 24 hr (Figure S4). To determine whether Fgfr activation is required for heart regeneration, we exposed wild-type and *hsp70:dn-fgfr1* clutchmates to 7, 14, and 30 days of daily heat induction after ventricular resection surgery. Formation of differentiated myocardium was assessed by ISH using a probe for *cmlc2*. *hsp70:dn-fgfr1* animals showed no differences from wild-types by 7 dpa (n = 6 animals) but presented slightly larger wounds

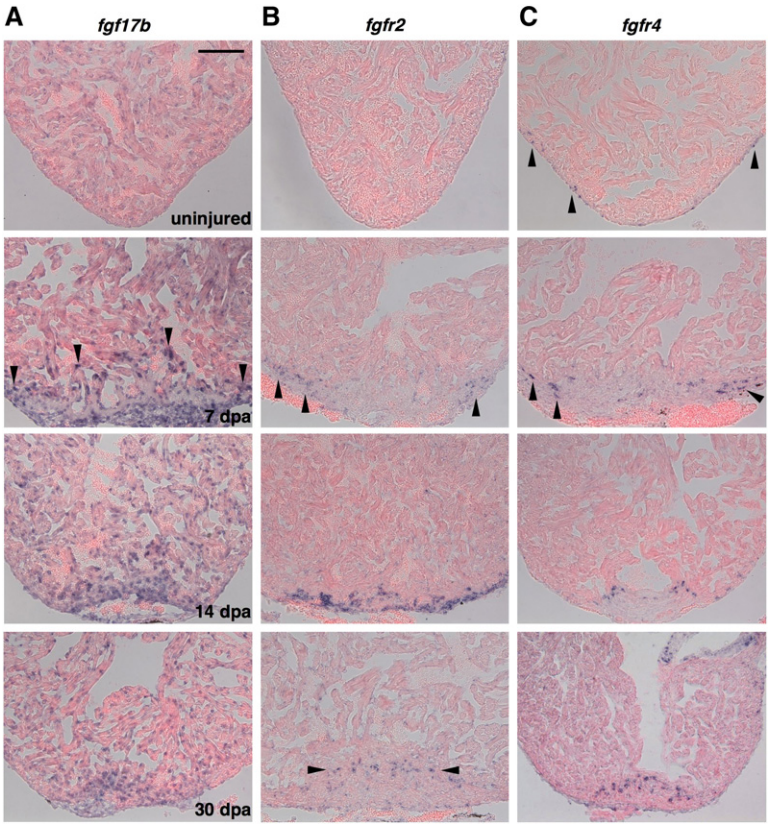

Figure 5. Expression of *fgf17b*, *fgfr2*, and *fgfr4* during Heart Regeneration

(A) Expression of *fgf17b* in the uninjured, 7, 14, and 30 dpa heart visualized by ISH. Weak, perinuclear expression was observed in uninjured ventricular CMs. Starting at 7 dpa, myofibers at the apical edge of the regenerate showed enhanced *fgf17b* expression (arrowheads), as did other cells within and around the injury. This augmentation persisted in regenerating muscle through 30 dpa.

(B) Expression of *fgfr2* during heart regeneration. While the uninjured ventricle showed no *fgfr2* expression, epicardial cells induced *fgfr2* upon entering the wound at 7 dpa (arrowheads), where expression was strongest at 14 dpa. By 30 dpa, faint expression was observed in isolated cells within the regenerate (arrowheads).

(C) *fgfr4* is expressed in a small number of epicardial or subepicardial cells on the uninjured ventricle (arrowheads) and induced in cells adjacent to regenerating muscle at 7 dpa and 14 dpa. *fgfr4*-expressing cells remain detectable in the regenerate by 30 dpa; in this image, *fgfr4* expression in the valve can also be observed (upper right corner). Scale bar = 100 μm.

(*cmlc2*-negative tissue) by 14 dpa (n = 12). While the majority of wild-type animals restored a contiguous *cmlc2*-positive ventricular wall by 30 dpa, *hsp70:dn-fgfr1* ventricles continued to display prominent wounds (n = 20; Figure 6A). A second, independent line of *hsp70:dn-fgfr1* zebrafish showed identical defects at 30 dpa (data not shown). Instead of completing regeneration, transgenic fish retained substantial fibrin deposits and developed large, collagen-rich scars. Analysis of later times postinjury indicated that the fibrin was eventually replaced by additional scar tissue (data not shown). By contrast, wild-type ventricles displaced wound fibrin with myocardium by 30 dpa and displayed only small collagen deposits (n = 14; Figure 6B). These results demonstrate that heart regeneration is an Fgf-dependent process.

To determine whether this regenerative failure was caused by defects in epicardial-derived cells, we assessed *tbx18* expression at 14 and 30 dpa in *hsp70:dn-fgfr1* animals. In the absence of Fgf signaling, *tbx18*-positive epicardial cells enveloped the wound normally by 14 dpa. However, instead of integrating into the clot or into regenerating muscle, these cells accumulated on the periphery of the apex (n = 9; Figure 6C). This phenotype did not result from developmental delay, as *tbx18*-positive cells continued to remain on the periphery by 30 dpa (n = 10). To determine the effects of this deficiency on the epicardial-derived coronary plexus, we assessed *hsp70:dn-fgfr1*; *fli1:EGFP* double transgenics. Vessels were observed in some cases at the apical edge of the clot material in these animals. Strikingly, we found little or no organized endothelium within the wound and adjacent to muscle at 14 or 30 dpa, indicating a severe failure in coronary neovascularization (n = 8; Figure 6D). Consistent with our failure to detect myocardial expression of *fgfr* genes during regeneration, assays for *tbx20* expression and RFP fluorescence in injured *hsp70:dn-fgfr1* or *hsp70:dn-fgfr1;cmlc2:nRFP* hearts at 14 dpa indicated no gross disruption of the adult myocardial differentiation program per se (n = 8; Figure S5).

Our findings demonstrate that Fgf signaling is seminal to the regenerative capacity of the zebrafish heart. This pathway, ostensibly stimulated in Fgfr2/4-expressing epicardial cells by myocardial Fgf17b, is essential to promote epicardial EMT into regenerating myocardium. Without this recruitment of epicardial cells, coronary neovascularization fails, limiting myocardial regeneration and enabling scar formation.

DISCUSSION

Zebrafish Heart Regeneration Is Initiated by Progenitor Cells

Our experiments reveal several new mechanistic insights into zebrafish heart regeneration, from which we propose a model (Figure 7). First, developmental timing assays using transgenic reporters of contractile gene expression

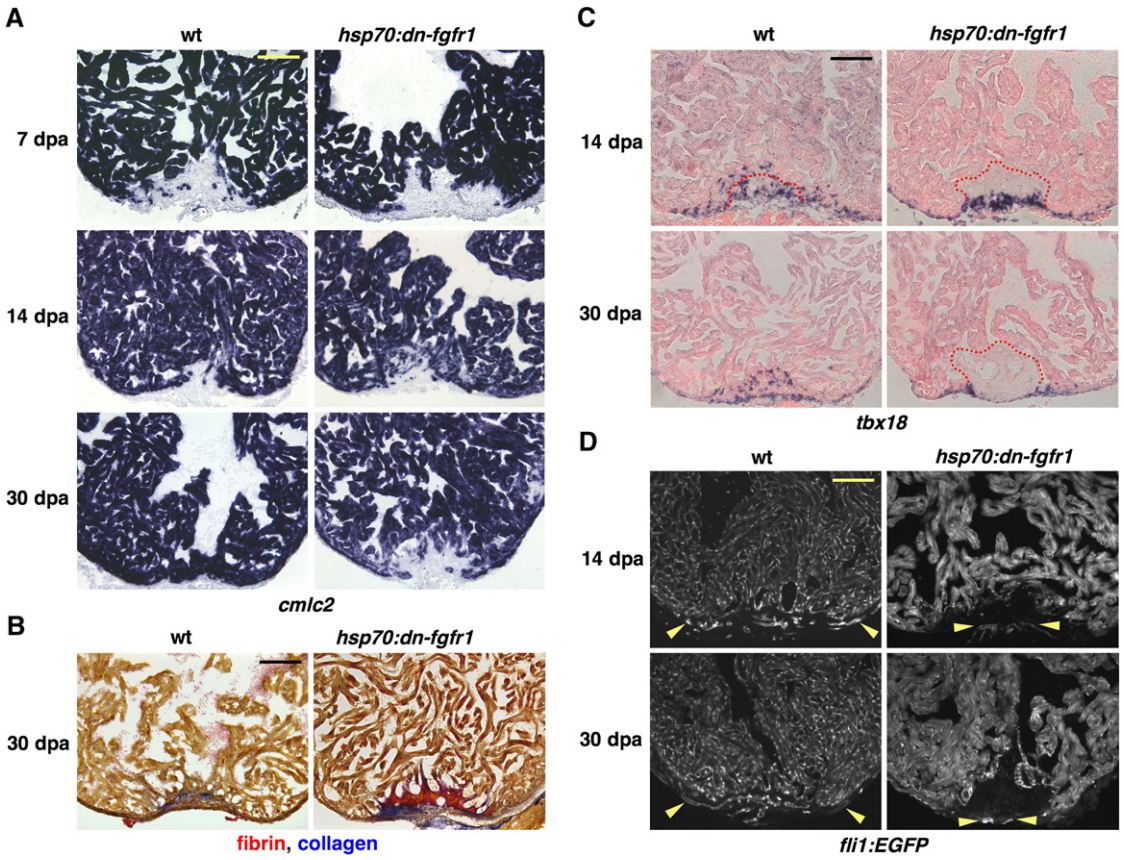

Figure 6. Fgfr Inhibition Blocks Epicardial EMT, Disrupting Coronary Neovascularization and Arresting Regeneration

(A) *cmlc2* expression at 7, 14, and 30 dpa in heat-induced wild-type and *hsp70:dn-fgfr1* zebrafish. Transgenic animals arrested regeneration of *cmlc2*-positive differentiated muscle around 14 dpa, leaving a large wound by 30 dpa.

(B) Thirty dpa hearts stained with acid fuchsin-orange G (AFOG). Wild-type ventricles display small deposits of scar tissue (blue) within a restored myocardial wall, while *hsp70:dn-fgfr1* hearts retain large amounts of fibrin (orange) and collagen (blue).

(C) Wild-type and *hsp70:dn-fgfr1* ventricles at 14 and 30 dpa, stained for *tbx18* expression by ISH. Wild-type *tbx18*-positive cells integrate into the regenerating muscle, but *hsp70:dn-fgfr1 tbx18*-positive cells fail to integrate and accumulate at the apical edge of the wound. Clot material is outlined in red.

(D) Wild-type *fli1:EGFP* and *hsp70:dn-fgfr1; fli1:EGFP* ventricles at 14 and 30 dpa. Wild-type regenerates are well vascularized (region within arrowheads). By contrast, transgenic wounds developed little or no organized endothelial structures in the vicinity of muscle. Occasionally, vessels were seen on the periphery of the wound, as indicated by arrowheads in these ventricles. *hsp70:dn-fgfr1* ventricles also display heat-induced fluorescence from the *EGFP*-tagged transgene. Scale bar = 100 μm.

revealed that regeneration is initiated predominantly by undifferentiated progenitor cells. Beginning at 3–4 days of injury, these cells localize at the apical edge of existing myocardium, activate precardiac and contractile gene expression, and proliferate. Thus, formation of the blastema constitutes the first stage of heart regeneration.

This mechanism is somewhat unexpected, as the simplest explanation from previous studies was that existing CMs divide in response to injury without changing contractile status. That same interpretation is inferred from studies of cultured newt CMs, a subpopulation of which divide in culture with no reported change in contractile gene expression (Bettencourt-Dias et al., 2003). We speculate that injury-related signals are insufficient to stimulate meaningful proliferation from existing adult zebrafish cardiac muscle and that progenitor cells contribute CMs with increased mitotic capacity. Determining signals that assist these progenitor cells to naturally assimilate with existing myofibers, mature, and proliferate will help to understand how myocardial regeneration can best be supported by progenitor cells in mammalian cardiac biology and disease.

During urodele lens, tail, and limb regeneration, there is evidence that structural cells lose functional characteristics or dedifferentiate to contribute progenitor cells to the blastema (Eguchi et al., 1974; Lo et al., 1993; Echeverri and Tanaka, 2002). Although we used a sensitive developmental timing assay capable of detecting myocardial dedifferentiation, we did not identify CMs with a prolonged arrest of contractile gene expression after injury. Furthermore, the apical edge of the regenerate expressed

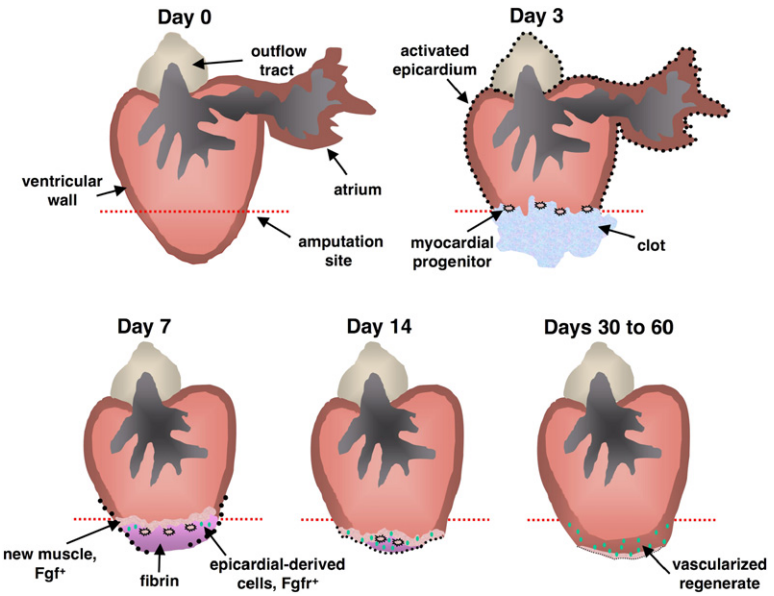

Figure 7. Model for Zebrafish Heart Regeneration

Resection of the ventricular apex stimulates rapid expansion of the entire epicardium by 3 dpa (black dots), at which time myocardial progenitor cells first originate in the wound, express precardiac markers, and associate with existing muscle. By 7 dpa, *raldh2*/*tbx18*-positive epicardial cells begin to surround and invade the wound. Meanwhile, there is continued seeding, maturation, and proliferation of myocardial progenitor cells, contributing the first layers of new muscle (stage 1).

To coordinate these epicardial and myocardial events, regenerating myocardium synthesizes Fgf17b and possibly other factors with the potential to recruit Fgfr2/Fgfr4-presenting epicardial cells. Epicardial-derived cells undergo EMT in response and vascularize the regenerate (green dots). Presence of new coronary vasculature by 14 dpa extends progenitor cell activity and facilitates restoration and expansion of the ventricular wall (stage 2).

increased levels of the myocardial differentiation activators *nkx2.5*, *tbx20*, *hand2*, *tbx5*, and Mef2. Therefore, while our data do not rule out rare or rapid dedifferentiation events, they better support the idea that myocardial progenitors originate primarily from an existing or injury-activated reserve. Potential sources for these cells, first identifiable in our experiments by their expression of *hand2*, may be similar to identified mammalian cardiac progenitor cell populations or could even include cardiac cell types like epicardium or endocardium. Interestingly, we have assessed expression of *islet1*, *islet2*, and *islet3*, as well as *kita* and *kitb*, during heart regeneration but found no detectable expression by ISH at 7 dpa (unpublished observations). Continued pursuit of unique markers for zebrafish myocardial progenitor cells and application of Cre-mediated genetic lineage labeling techniques (Cai et al., 2003; Meilhac et al., 2003) should help to address the intriguing question of how these cells arise.

Cardiac Injury Causes Organ-Wide Epicardial Augmentation

Second, we identified immediate and organ-wide transmission and reception of the cardiac injury signal in epicardial tissues. By 3 dpa, an abundance of developmentally activated epicardial tissue covered the heart, enveloping the wound by 7–14 dpa. Very little is known about the function of the epicardium encasing the adult vertebrate heart. Our results show that the adult zebrafish epicardium is a highly plastic and responsive structure, performing analogously to the classic regeneration epidermis that revitalizes an amputated appendage.

How cardiac injury augments the entire epicardial layer is unknown. Organ-wide injury responses are known to occur during other displays of regeneration. For example, in the adult mammalian liver, partial hepatectomy stimulates proliferation in approximately 95% of remaining hepatocytes (Taub, 2004). Recently, it was found that the efficacy of liver regeneration is modified through feedback mechanisms that gauge its ability to produce bile acids (Huang et al., 2006). An analogous idea is that myocardial integrity is somehow assessed biochemically by its output and that a feedback mechanism may have an initial organ-wide effect to increase epicardial tissue.

New epicardial cells could either be derived by stimulation of the quiescent adult epicardium or from a progenitor cell population transformed by injury. Relevant to the latter, it is interesting that the spatial and temporal properties of the regenerative epicardial response mimic the basal-to-apical manner in which an epithelial sheet first emerges from the proepicardial organ (PEO) at the embryonic atrioventricular (AV) junction to cover the growing cardiac chambers (Reese et al., 2002). Therefore, it is possible that there is an analogous structure to the PEO located at the adult AV junction, one that can generate proliferative, migratory epicardial tissue in response to injury. In any case, the large epicardial pool that is created after injury ostensibly expedites identification of the damaged muscle and optimizes subsequent EMT and neovascularization.

Targeted, Fgf-Dependent Epicardial EMT Maintains Heart Regeneration

Third, our study revealed a mechanism by which the activated epicardium supports the activities of cardiac progenitor cells, constituting the second stage of regeneration (Figure 7). Within two weeks after injury, epicardial cells expressing *raldh2* and *tbx18* localize to the wound. Here, not only do these cells provide cover for the naked myocardium, but a subpopulation retains *tbx18* expression, undergoes EMT, penetrates the regenerate, and ultimately settles many cell layers deep into the muscle to establish new vascular tissue.

We have found that epicardial cells express Fgf receptors as they approach the wound, and moreover, Fgf signaling is essential for their recruitment into regenerating muscle. While multiple sources and forms of Fgfs might be present during regeneration, Fgf17b synthesis is increased in wounded/regenerating myocardium from 7 to 30 dpa and is an excellent candidate to attract epicardial-derived cells expressing *fgfr2* and/or *fgfr4*. Such coordination of epicardial and myocardial activities by Fgf signaling to vascularize new CMs represents a provocative mechanism to maintain and extend heart regeneration after the blastema is formed. It is likely that such an interaction represents one arm of a regulatory loop involving numerous signals between epicardium and myocardium.

During embryonic heart development, the transcription factor FOG2 is required in the growing myocardium for the formation of coronary vasculature (Tevosian et al., 2000). This finding demonstrated that normal development of epicardial-derived tissues requires signals from the myocardium. Furthermore, in addition to in vitro effects of Fgfs on epicardial EMT mentioned earlier, recent studies indicate that experimentally augmenting the concentration of Fgfs in the myocardium of the developing avian heart by retroviral expression can increase the density of coronary vessels (Pennisi and Mikawa, 2005). Finally, a recent study showed that Fgf signaling is required for normal vascularization of the developing murine heart, possibly through interactions with Vegf and Hedgehog signaling pathway members (Lavine et al., 2006). The embryonic heart is a highly tractable model for understanding cardiogenesis, and we expect that studies of embryonic heart development and adult heart regeneration will together yield valuable comparisons. Our current study illustrates that the regenerating heart can recall signaling pathways essential during its embryonic manifestation.

Myocardial Regeneration Utilizes a Vascularized Niche

We have found that regeneration by zebrafish myocardial progenitor cells is optimized within a fostering niche that includes a regeneration epidermis and an abundant vascular supply. Blood vessels, as well as specific components of endothelial cells, promote developmental activity of neural stem cells (Shen et al., 2004). In addition, proliferation and function of adult pancreatic β cells are nurtured by vascular endothelial components such as laminins (Nikolova et al., 2006). It is thus possible that specific properties of coronary vessels, in addition to nutritional provision, promote regenerative cardiogenesis.

Our results show that an elaborate sequence of organ-wide and local responses by epicardial and myocardial cells orchestrates the vascularized niche. It is tempting to speculate that the ability to mobilize epicardial cells and cultivate such a cardiogenic environment is a primary reason why zebrafish, as opposed to other laboratory models, effectively regenerate myocardium. Indeed, mammalian hearts typically show insufficient neovascularization after myocardial infarction. Experimental attempts to modify this deficiency are underway, including delivery of growth factors or bone marrow-derived cells that may promote neovascularization in a paracrine manner or become incorporated into vessels (reviewed in Dimmeler et al., 2005). Success in these pursuits or by directly utilizing epicardial cells or their progenitors could prove favorable for encouraging regeneration from mammalian cardiac progenitor cells.

EXPERIMENTAL PROCEDURES

Zebrafish and Ventricular Resection

Outbred Ekkwill strain (EK) or EK/*AB mixed background zebrafish 6–12 months of age were used for ventricular resection surgeries. As described previously, ~20% of ventricular muscle was removed at the apex with iridectomy scissors (Poss et al., 2002). To visualize specific cell types, we used *cmlc2:nuc-DsRed2* (*cmlc2:nRFP*; Mably et al., 2003), *cmlc2:EGFP* (Burns et al., 2005), *fli1:EGFP* (Lawson and Weinstein, 2002), *flk1:EGFP* (Jin et al., 2005), or *β-actin 2:EGFP* (Traver et al., 2003) transgenic strains or crosses between the strains to generate double transgenics. All transgenic strains were analyzed as heterozygotes in our experiments. All animal procedures were performed in accordance with Duke University guidelines.

Adult Heat-Induction Experiments

Male *hsp70:dn-fgfr1* transgenic and wild-type control animals from the same parents were injured, allowed overnight recovery from surgery at room temperature, and then exposed daily to a transient, automated increase in temperature from 26°C to 38°C (Lee et al., 2005). With this protocol, animals remained at 38°C for ~60 min each day. All heart collections were performed 4–5 hr after heat shock. The *hsp70:dn-fgfr1* construct is predicted to heterodimerize with all Fgfr subtypes, thereby competitively blocking signaling downstream of all Fgfr subtypes.

Histological Methods

ISH on cryosections of paraformaldehyde-fixed hearts was performed using digoxygenin-labeled cRNA probes as described (Poss et al., 2002). For double ISH, digoxygenin-labeled *fgfr4* cRNA and fluorescein-labeled *tbx18* cRNA probes were synthesized using DIG-dUTP and fluorescein-dUTP (Roche). The TSA biotin system and the TSA Plus fluorescence system (Perkin Elmer) were used for amplifying the signal. Whole-mount ISH on intact hearts (performed for experiments in Figures 3A and 3B) was performed as described (Poss et al., 2000). Acid fuchsin-orange G staining was performed as described (Poss et al., 2002). For BrdU-labeling experiments, animals were injected intraperitoneally with ~0.05 ml of a 2.5 mg/ml solution of BrdU dissolved in buffered Hank's solution. BrdU was injected once every 24 hr for 3 days prior to heart collection, and immunodetection of BrdU after ISH was performed as described (Lee et al., 2005). Polyclonal antibodies against Mef2 (Santa Cruz Biotechnology) and DsRed (Clontech) were used for immunofluorescence analyses.

Supplemental Data

Supplemental Data include five figures and one table and can be found with this article online at http://www.cell.com/cgi/content/full/127/3/607/DC1/.

ACKNOWLEDGMENTS

We thank Y. Gibert, H. Grandel, A. Nechiporuk, H. Okamoto, I. Scott, H. Takeda, and D. Yelon for in situ probes; S. Jin and D. Stainier for *flk1:EGFP* zebrafish; the Zebrafish International Resource Center for *fli1:EGFP* zebrafish; C. Wheeler and V. Tsang for excellent zebrafish care; and T. Camp, A. McGraw, T. Okubo, and L. Wilson for helping

to establish assays. We thank B. Hogan, A. Nechiporuk, S. Odelberg, D. Yelon, L. Zon, and Poss lab members for helpful comments on the manuscript. This work was supported by grants to K.D.P. from NIH, American Heart Association, March of Dimes, and the Whitehead Foundation.

Received: March 27, 2006
Revised: July 8, 2006
Accepted: August 23, 2006
Published: November 2, 2006

REFERENCES

Akimoto, A., Wada, H., and Hayashi, S. (2005). Enhancer trapping with a red fluorescent protein reporter in Drosophila. Dev. Dyn. *233*, 993–997.

Baird, G.S., Zacharias, D.A., and Tsien, R.Y. (2000). Biochemistry, mutagenesis, and oligomerization of DsRed, a red fluorescent protein from coral. Proc. Natl. Acad. Sci. USA *97*, 11984–11989.

Beltrami, A.P., Barlucchi, L., Torella, D., Baker, M., Limana, F., Chimenti, S., Kasahara, H., Rota, M., Musso, E., Urbanek, K., et al. (2003). Adult cardiac stem cells are multipotent and support myocardial regeneration. Cell *114*, 763–776.

Bettencourt-Dias, M., Mittnacht, S., and Brockes, J.P. (2003). Heterogeneous proliferative potential in regenerative adult newt cardiomyocytes. J. Cell Sci. *116*, 4001–4009.

Bevis, B.J., and Glick, B.S. (2002). Rapidly maturing variants of the Discosoma red fluorescent protein (DsRed). Nat. Biotechnol. *20*, 83–87.

Brockes, J.P., and Kumar, A. (2005). Appendage regeneration in adult vertebrates and implications for regenerative medicine. Science *310*, 1919–1923.

Burns, C.G., Milan, D.J., Grande, E.J., Rottbauer, W., MacRae, C.A., and Fishman, M.C. (2005). High-throughput assay for small molecules that modulate zebrafish embryonic heart rate. Nat. Chem. Biol. *1*, 263–264.

Cai, C.L., Liang, X., Shi, Y., Chu, P.H., Pfaff, S.L., Chen, J., and Evans, S. (2003). Isl1 identifies a cardiac progenitor population that proliferates prior to differentiation and contributes a majority of cells to the heart. Dev. Cell *5*, 877–889.

Cao, Y., Zhao, J., Sun, Z., Zhao, Z., Postlethwait, J., and Meng, A. (2004). fgf17b, a novel member of Fgf family, helps patterning zebrafish embryos. Dev. Biol. *271*, 130–143.

Chen, J.N., and Fishman, M.C. (1996). Zebrafish tinman homolog demarcates the heart field and initiates myocardial differentiation. Development *122*, 3809–3816.

Chen, J.N., Haffter, P., Odenthal, J., Vogelsang, E., Brand, M., van Eeden, F.J., Furutani-Seiki, M., Granato, M., Hammerschmidt, M., Heisenberg, C.P., et al. (1996). Mutations affecting the cardiovascular system and other internal organs in zebrafish. Development *123*, 293–302.

Dettman, R.W., Denetclaw, W., Jr., Ordahl, C.P., and Bristow, J. (1998). Common epicardial origin of coronary vascular smooth muscle, perivascular fibroblasts, and intermyocardial fibroblasts in the avian heart. Dev. Biol. *193*, 169–181.

Dimmeler, S., Zeiher, A.M., and Schneider, M.D. (2005). Unchain my heart: the scientific foundations of cardiac repair. J. Clin. Invest. *115*, 572–583.

Echeverri, K., and Tanaka, E.M. (2002). Ectoderm to mesoderm lineage switching during axolotl tail regeneration. Science *298*, 1993–1996.

Eguchi, G., Abe, S.I., and Watanabe, K. (1974). Differentiation of lens-like structures from newt iris epithelial cells in vitro. Proc. Natl. Acad. Sci. USA *71*, 5052–5056.

Griffin, K.J., Stoller, J., Gibson, M., Chen, S., Yelon, D., Stainier, D.Y., and Kimelman, D. (2000). A conserved role for H15-related T-box transcription factors in zebrafish and Drosophila heart formation. Dev. Biol. *218*, 235–247.

Huang, W., Ma, K., Zhang, J., Qatanani, M., Cuvillier, J., Liu, J., Dong, B., Huang, X., and Moore, D.D. (2006). Nuclear receptor-dependent bile acid signaling is required for normal liver regeneration. Science *312*, 233–236.

Jin, S.W., Beis, D., Mitchell, T., Chen, J.N., and Stainier, D.Y. (2005). Cellular and molecular analyses of vascular tube and lumen formation in zebrafish. Development *132*, 5199–5209.

Keegan, B.R., Feldman, J.L., Begemann, G., Ingham, P.W., and Yelon, D. (2005). Retinoic acid signaling restricts the cardiac progenitor pool. Science *307*, 247–249.

Kraus, F., Haenig, B., and Kispert, A. (2001). Cloning and expression analysis of the mouse T-box gene Tbx18. Mech. Dev. *100*, 83–86.

Laugwitz, K.L., Moretti, A., Lam, J., Gruber, P., Chen, Y., Woodard, S., Lin, L.Z., Cai, C.L., Lu, M.M., Reth, M., et al. (2005). Postnatal isl1+ cardioblasts enter fully differentiated cardiomyocyte lineages. Nature *433*, 647–653.

Lavine, K.J., White, A.C., Park, C., Smith, C.S., Choi, K., Long, F., Hui, C.C., and Ornitz, D.M. (2006). Fibroblast growth factor signals regulate a wave of Hedgehog activation that is essential for coronary vascular development. Genes Dev. *20*, 1651–1666.

Lawson, N.D., and Weinstein, B.M. (2002). In vivo imaging of embryonic vascular development using transgenic zebrafish. Dev. Biol. *248*, 307–318.

Lee, Y., Grill, S., Sanchez, A., Murphy-Ryan, M., and Poss, K.D. (2005). Fgf signaling instructs position-dependent growth rate during zebrafish fin regeneration. Development *132*, 5173–5183.

Lo, D.C., Allen, F., and Brockes, J.P. (1993). Reversal of muscle differentiation during urodele limb regeneration. Proc. Natl. Acad. Sci. USA *90*, 7230–7234.

Mably, J.D., Mohideen, M.A., Burns, C.G., Chen, J.N., and Fishman, M.C. (2003). heart of glass regulates the concentric growth of the heart in zebrafish. Curr. Biol. *13*, 2138–2147.

Meilhac, S.M., Kelly, R.G., Rocancourt, D., Eloy-Trinquet, S., Nicolas, J.F., and Buckingham, M.E. (2003). A retrospective clonal analysis of the myocardium reveals two phases of clonal growth in the developing mouse heart. Development *130*, 3877–3889.

Morabito, C.J., Dettman, R.W., Kattan, J., Collier, J.M., and Bristow, J. (2001). Positive and negative regulation of epicardial-mesenchymal transformation during avian heart development. Dev. Biol. *234*, 204–215.

Moss, J.B., Xavier-Neto, J., Shapiro, M.D., Nayeem, S.M., McCaffery, P., Drager, U.C., and Rosenthal, N. (1998). Dynamic patterns of retinoic acid synthesis and response in the developing mammalian heart. Dev. Biol. *199*, 55–71.

Nikolova, G., Jabs, N., Konstantinova, I., Domogatskaya, A., Tryggvason, K., Sorokin, L., Fassler, R., Gu, G., Gerber, H.P., Ferrara, N., et al. (2006). The vascular basement membrane: a niche for insulin gene expression and Beta cell proliferation. Dev. Cell *10*, 397–405.

Oberpriller, J.O., and Oberpriller, J.C. (1974). Response of the adult newt ventricle to injury. J. Exp. Zool. *187*, 249–253.

Oh, H., Bradfute, S.B., Gallardo, T.D., Nakamura, T., Gaussin, V., Mishina, Y., Pocius, J., Michael, L.H., Behringer, R.R., Garry, D.J., et al. (2003). Cardiac progenitor cells from adult myocardium: homing, differentiation, and fusion after infarction. Proc. Natl. Acad. Sci. U.S.A. *100*, 12313–12318.

Olivey, H.E., Compton, L.A., and Barnett, J.V. (2004). Coronary vessel development: the epicardium delivers. Trends Cardiovasc. Med. *14*, 247–251.

Olsen, S.K., Li, J.Y., Bromleigh, C., Eliseenkova, A.V., Ibrahimi, O.A., Lao, Z., Zhang, F., Linhardt, R.J., Joyner, A.L., and Mohammadi, M.

(2006). Structural basis by which alternative splicing modulates the organizer activity of FGF8 in the brain. Genes Dev. *20*, 185–198.

Pennisi, D.J., and Mikawa, T. (2005). Normal patterning of the coronary capillary plexus is dependent on the correct transmural gradient of FGF expression in the myocardium. Dev. Biol. *279*, 378–390.

Poss, K.D., Shen, J., Nechiporuk, A., McMahon, G., Thisse, B., Thisse, C., and Keating, M.T. (2000). Roles for Fgf signaling during zebrafish fin regeneration. Dev. Biol. *222*, 347–358.

Poss, K.D., Wilson, L.G., and Keating, M.T. (2002). Heart regeneration in zebrafish. Science *298*, 2188–2190.

Raya, A., Koth, C.M., Buscher, D., Kawakami, Y., Itoh, T., Raya, R.M., Sternik, G., Tsai, H.J., Rodriguez-Esteban, C., and Izpisua-Belmonte, J.C. (2003). Activation of Notch signaling pathway precedes heart regeneration in zebrafish. Proc. Natl. Acad. Sci. USA *100* (*Suppl 1*), 11889–11895.

Reddien, P.W., and Sanchez Alvarado, A. (2004). Fundamentals of planarian regeneration. Annu. Rev. Cell Dev. Biol. *20*, 725–757.

Reese, D.E., Mikawa, T., and Bader, D.M. (2002). Development of the coronary vessel system. Circ. Res. *91*, 761–768.

Rubart, M., and Field, L.J. (2006). Cardiac regeneration: repopulating the heart. Annu. Rev. Physiol. *68*, 29–49.

Scadding, S.R. (1977). Phylogenic distribution of limb regeneration capacity in adult *Amphibia*. J. Exp. Zool. *202*, 57–68.

Shen, Q., Goderie, S.K., Jin, L., Karanth, N., Sun, Y., Abramova, N., Vincent, P., Pumiglia, K., and Temple, S. (2004). Endothelial cells stimulate self-renewal and expand neurogenesis of neural stem cells. Science *304*, 1338–1340.

Shizuru, J.A., Negrin, R.S., and Weissman, I.L. (2005). Hematopoietic stem and progenitor cells: clinical and preclinical regeneration of the hematolymphoid system. Annu. Rev. Med. *56*, 509–538.

Stainier, D.Y., Fouquet, B., Chen, J.N., Warren, K.S., Weinstein, B.M., Meiler, S.E., Mohideen, M.A., Neuhauss, S.C., Solnica-Krezel, L., Schier, A.F., et al. (1996). Mutations affecting the formation and function of the cardiovascular system in the zebrafish embryo. Development *123*, 285–292.

Taub, R. (2004). Liver regeneration: from myth to mechanism. Nat. Rev. Mol. Cell Biol. *5*, 836–847.

Tevosian, S.G., Deconinck, A.E., Tanaka, M., Schinke, M., Litovsky, S.H., Izumo, S., Fujiwara, Y., and Orkin, S.H. (2000). FOG-2, a cofactor for GATA transcription factors, is essential for heart morphogenesis and development of coronary vessels from epicardium. Cell *101*, 729–739.

Traver, D., Paw, B.H., Poss, K.D., Penberthy, W.T., Lin, S., and Zon, L.I. (2003). Transplantation and in vivo imaging of multilineage engraftment in zebrafish bloodless mutants. Nat. Immunol. *4*, 1238–1246.

Verkhusha, V.V., Otsuna, H., Awasaki, T., Oda, H., Tsukita, S., and Ito, K. (2001). An enhanced mutant of red fluorescent protein DsRed for double labeling and developmental timer of neural fiber bundle formation. J. Biol. Chem. *276*, 29621–29624.

Verkhusha, V.V., Kuznetsova, I.M., Stepanenko, O.V., Zaraisky, A.G., Shavlovsky, M.M., Turoverov, K.K., and Uversky, V.N. (2003). High stability of Discosoma DsRed as compared to Aequorea EGFP. Biochemistry *42*, 7879–7884.

Wagers, A.J., Sherwood, R.I., Christensen, J.L., and Weissman, I.L. (2002). Little evidence for developmental plasticity of adult hematopoietic stem cells. Science *297*, 2256–2259.

Wagner, G.P., and Misof, B.Y. (1992). Evolutionary modification of regenerative capability in vertebrates: a comparative study on teleost pectoral fin regeneration. J. Exp. Zool. *261*, 62–78.

Yelon, D., Ticho, B., Halpern, M.E., Ruvinsky, I., Ho, R.K., Silver, L.M., and Stainier, D.Y. (2000). The bHLH transcription factor hand2 plays parallel roles in zebrafish heart and pectoral fin development. Development *127*, 2573–2582.